8   Photon Beam Transport and Diagnostics

Synopsis

FERMI@Elettra includes two separate undulator sections named FEL-1 and FEL-2 delivering radiation in the $100 \div 40$ nm and $40 \div 10$ nm ranges, respectively. For FEL-1 a $50 \div 100$ fs pulse is delivered with a peak power of about 1-5 GW, and $\sim 10^{14}$ photons per pulse are expected. FEL-2 is characterized by a 200 fs pulse carrying about 1 GW and 10^{12} (fresh bunch mode).

In order to characterize, select, and carry the photon beam to the experimental endstations, a set of optical systems is placed after the undulators. Characteristics such as energy, energy resolution, pulse length, intensity, arrival time, polarization, and so on, are determined by means of several diagnostics located between the undulators and the experimental hall. Gas-based systems such as absorbers and intensity monitors are mounted within window-less in-vacuum sections. The gases intercepting the radiation axis serve as natural absorbers reducing the overall photon flux. Additionally, the gas ionization signal gives information about the relative intensity of the beam. A system of slits removes unwanted off-axis radiation mainly coming from spontaneous emission. It also works as an angular collimator making possible spectral-angular filtering.

At the entrance of the experimental hall radiation coming from each FEL impinges on a plane mirror used as a power absorbing element upstream of the more delicate elements along the beamlines. Moreover, this optical element is important from the radio-protection point of view.

In order to energetically and temporally characterize the radiation, an energy spectrograph, an angular distribution detector, and a temporal pulse length-measuring device are installed. The on-line spectrograph uses a variable line spacing plane grating that passes more than 95% of the radiation in reflection (zero order) to the following beamlines, while a small fraction of the total number of photons is diffracted within the orders of diffraction. The first order, in particular, is focused and directed onto a linear spatially sensitive detector to analyze the energy spectrum of the radiation, pulse by pulse. A two-dimensional detector characterizes the quality of the emitted radiation by checking the off-axis emission to give useful feedback for the undulator tuning. A streak camera determines the pulse length with a temporal resolution tentatively below 0.5 ps.

Proper beamline designs are currently under study for the different experiments foreseen for FERMI@ Elettra. A main design goal is the possibility of serving some of the endstations with light coming from both FELs (not simultaneously). Moreover, the optics take into account the fact that the effective photon source moves longitudinally as the emission energy is varied.

Different traditional monochromator schemes are considered, and a detailed study is in progress to determine the best configuration for the needs of the different experiments. In addition, a scheme for a time preserving monochromator is described and discussed.

8.1   Introduction

Two free-electron-lasers are employed to deliver radiation from 12 to 124 eV with bandwidths of 40 and 15 meV (for FEL-1 and 2 respectively). Some experiments can work with this level of energy resolution, and keep the pulse length as short as possible. In those cases in which a higher degree of monochromatization is needed, the inevitable drawback of a lengthening the pulse length must be faced. Consequently, different designs are adopted for the two cases: high-energy resolution and short-pulses beamlines. These lines are currently being designed according to the specific users' needs. Another design takes contemplates focusing of the FEL radiation directly on the samples in the endstations.

The major design challenge is the high peak power of the FEL pulses (up to several gigawatts) that imposes severe constrains on the beamline design and on the optical coatings. Moreover, the pulsed structure of the radiation calls for proper diagnostics to characterize the pulse length, spectral profile, and intensity. These diagnostics at first serve as tools for optimizing the machine performance, and include also more specific tools as radiation angular distribution detectors.

8.2   Differences between FEL and Synchrotron Radiation

The very high peak energy arriving on the optical elements, together with the extremely short pulse length, is the main difference between FEL and synchrotron radiation (SR). This difference calls for modifications of usual synchrotron beamline designs as well as the choice of proper materials. The peak energy density from the FEL is four to five orders of magnitude higher than in undulator beams at 3rd generation synchrotron facilities. Such energy, delivered in sub-picosecond pulses, creates a large number of ionized surface atoms on the optical elements (as well as on the samples) before de-excitation processes can take place. As a consequence, desorption (ablation) of surface atoms may occur. Recent first tests carried out at 12 eV on silicon-, carbon-, and gold-coated mirrors carried on at TTF-FEL in DESY [1] can help meet this new challenge (not present at SR facilities). To provide a conservative safety

margin the FERMI@Elettra beamlines are designed with peak fluences on optical elements that are 10 times lower that the damage thresholds verified for the chosen optical materials. Furthermore, focusing of the undispersed FEL radiation onto optical elements (slits included) is avoided in favor of grazing incidence angles on the optics. Finally, surface materials with as low ionization cross sections as possible are preferred.

8.2.1   Pulsed Structure

The radiation presents a pulsed structure with frequency of 10 – 50 Hz, and a pulse length of about $50 \div 200$ ps, with a peak power of $1 \div 5$ GW. The product of the pulse frequency and the pulse length, for the given peak energy determines the total delivered power. To safely estimate this value it is conservative to take 100 Hz as the frequency ($T = 10^{-2}$ s) for both FELs. For FEL-1 the product is about 10^{11}, while for FEL-2 it is 2.5×10^{10} in the fresh bunch mode. Therefore, the integral power load delivered on the first optical element of each beamline is about 1 W, or even less. One must add to this value the power due to the spontaneous emission of the undulator, as well as of the radiation emitted by the bending magnet used to deflect the beam out of the photon trajectory. Also in this case the pulsed nature of the radiation guarantees very low values for the average thermal load. These values are much smaller than what expected in typical SR beamlines, and consequently standard direct side cooling (with water) is appropriate (even if operations without cooling are possible).

Another major issue related to the pulsed structure is the fact that when this kind of radiation passes through a diffraction grating its time distribution is inevitably modified. This is a consequence of the different optical paths traveled by the individual photons within the same pulse. While the path difference is close to zero in the case of mirrors, it is no longer negligible in the case of diffractive elements. In this case (Figure 8.2.1) the rays traveling at opposite edges of the pulse travel different paths, this difference increases as the footprint of the photon beam on the grating surface is larger.
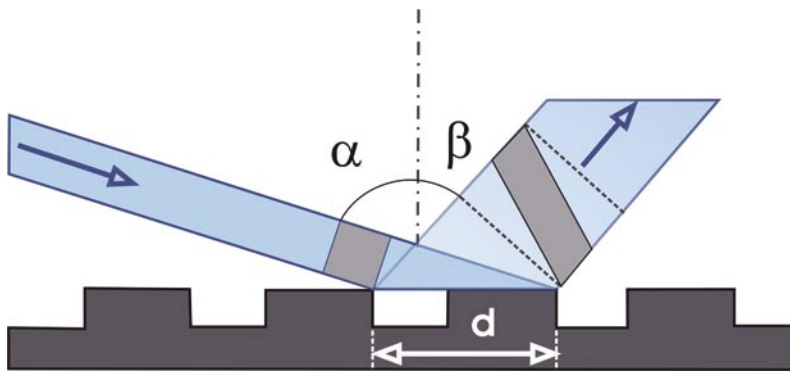

Figure 8.2.1:
Sketch of the path difference due to a single groove of a diffraction grating.

This path difference is equal to $Nd(\sin\alpha-\sin\beta)$, where N is the number of grooves lightened by the beam, d is the groove spacing, α and β are the incidence and diffraction angles, respectively. A pulse time duration enlargement Δt is determined and it can be roughly estimated to be equal to the path difference divided by the speed of light. According to the expected beam divergences and the necessary angles of incidence, Δt will range from 0.1 to 1 ps depending on the requested photon energy resolution. To be

more accurate a computer code able to simulate ray by ray the effect of this enlargement in the presence of mirrors or gratings for any source distribution has been created. An example is illustrated in Figure 8.2.2, where the effect of a high-resolution monochromator on the time profile of an incoming pulse (for two different pulse lengths) is simulated.
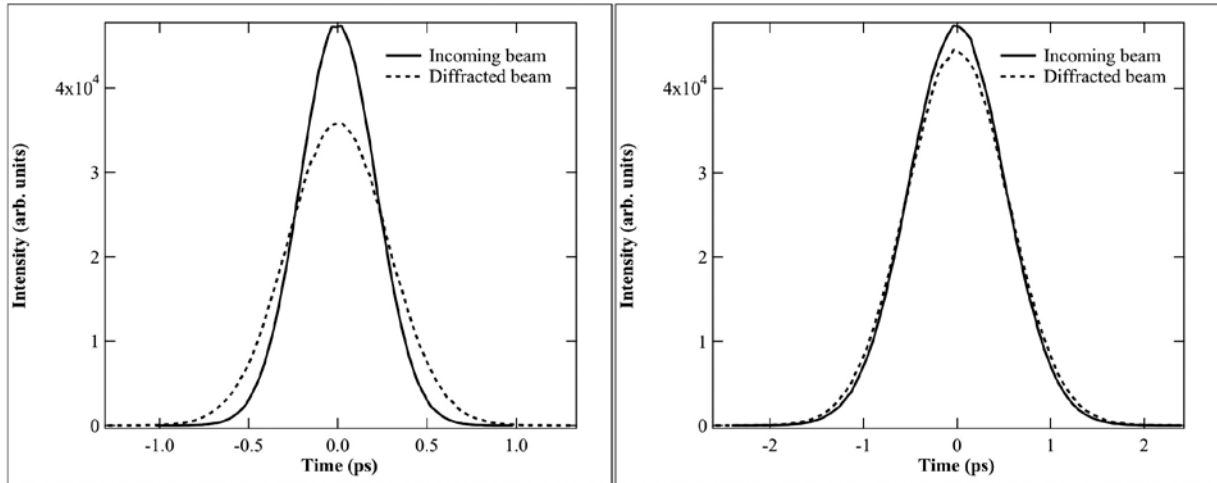

Figure 8.2.2:
Effect of a monochromator providing a bandwidth of less than 2 meV at 50 eV with a 1.2 ps pulse (right) and 0.5 ps pulse (left). The solid curves represent the incoming beam time profile, the dotted curves the diffracted beam profile.

Of course, one should always take into account the fact that a monochromatic beam can never be shorter then its transform limit, therefore, for a high resolution monochromator, thanks to the very low divergence of the beam, the effect of the enlargement due to the grating is negligible (or comparable) with respect to the natural time broadening due the lower energy bandwidth. The only case in which the grating effect is relevant is the case of low-resolution monochromators for FEL-1.

Clearly, when there is a strong demand very high-spectral purity of the photon beams in the experimental endstations, non-standard solutions must be adopted. One possibility is working with a double grating, time preserving monochromator (described in Section 8.4.3.2). This configuration uses two diffraction gratings mounted in opposite angle configurations: $\alpha \rightarrow \beta$ for the first one, $\beta \rightarrow \alpha$ for the second one (see Figure 8.2.3). In this way the longer path traveled by a photon on the first grating is compensated by traveling a shorter path on the second, and vice versa.
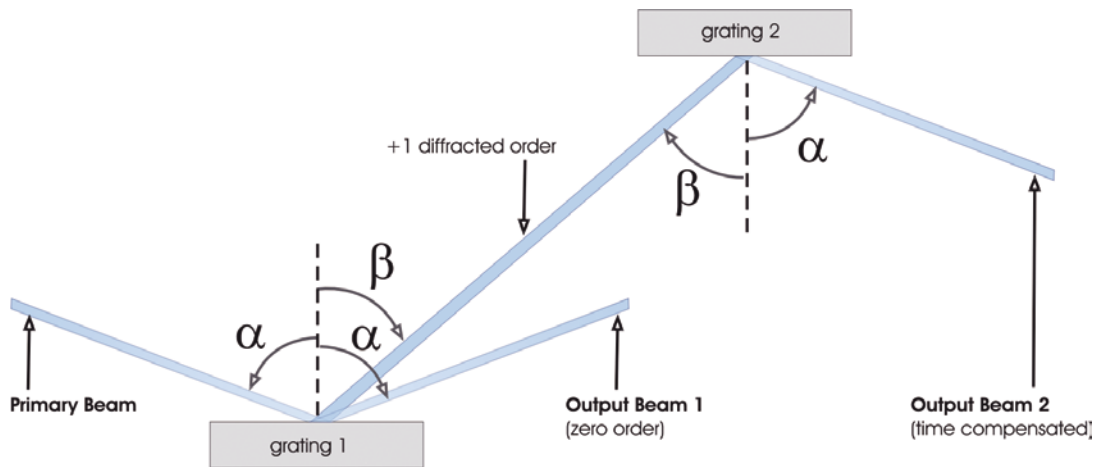
Figure 8.2.3:
Time-compensated monochromator working in α→β – β→α configuration.

8.2.2   High Powers

One of the main problems related with the very high peak brilliance is the power arriving on the optical elements in a very short temporal interval. Even if the average power is of the order of few Watts, requiring just a simple cooling system to prevent small mirror deformations, the peak power can go up to 10 GW in particular for FEL-1. To simulate the behavior of the FEL with enough margin to include variations of both pulse length and peak power, and to give a safe estimate of the behavior of the optics under such a high energy density, a box-shaped pulse has been used. In particular, for a 200 fs –pulse an energy of 2 mJ is delivered. Since the divergence of the beam is quite small, 50 μrad, it produces an energy density up to 0.2 J/cm^2 at 10 meters from the source. Such an energy density is higher than the damage threshold of several materials. Consequently grazing angles of incidence are used.

The absorbed energy density is also a key parameter, since the typical lattice disruption value of the order of 1 eV/atom must be not exceeded [2]. This quantity depends on a combination of parameters including the angle of incidence, the material attenuation length and atomic density, and the reflectivity. In particular, reducing the grazing angle of incidence introduces a competition between the reduction of the optical surface power load and the reduction of the geometrical dilution effect (due to the shorter penetration depth) leading to an increase of the load on the very first layers.

An experimental study was performed by A. Andrejczuk *et al.* [3], where the damage threshold of some materials was determined at 98 nm-wavelength and normal incidence. Shorter pulses or longer wavelength (for fixed pulse energy) determine a lower damage threshold. Moreover, the damage threshold is further reduced if the interval between two consecutive pulses is of the same order of the relaxation time of the materials [4]. Typically the ablation is a thermal process, and this means that it is expected to be lower on materials where the energy can be carried away rapidly [5].

There are some pre-process, before the ablation, which do not "destroy" the surface, but which can drastically deteriorate its optical properties. For instance, in bare silicon, the ablation threshold is 3.7 eV per atom for a 20 fs pulse at 780 nm (6.2 eV/atom for 500 fs) while the melting threshold is 2.6 and 5.4 eV/atom for 20 and 500 fs respectively [6]. In other materials (graphite or diamond) the damage threshold is from 2 to 4 times smaller than the ablation one [7].

Nevertheless, dedicated research efforts, including experiments, are required to improve understanding of the mechanisms contributing to ablation of optical surfaces, with the aim of properly defining the bulk and coating materials for the beamline elements.

Possible candidates for coating and/or bulk mirror materials are carbon and silicon, due to their sufficiently high damage thresholds and the possibility of realizing good quality optical surfaces with both materials. As a safety margin, designs with energy densities 10 times lower than the expected damage thresholds are preferred. The thresholds measured at 98 nm were redefined at different wavelengths simply by taking into account the differences in cross section at different energies. Also this assumption requires further study.

In table 8.2.1 the expected energy density 10 meters from the source and the necessary minimum angle of incidence to work within an energy density 10 times below the damage threshold are reported for an high density graphite coating. For FEL-2 there are no major constrains, while for FEL-1 great care must be used in selecting the position and angle of incidence for a mirror.

Table 8.2.1: **Expected energy density and maximum angle of incidence at 10 and 20 meters from the source for different possible machine configurations, for a carbon-coated mirror.**

FEL	Pulse Length	Peak Power	Energy density @ 10m	Safety incidence angle C coating (1/10 damage
1	200 fs	3 GW	180 mJ/cm²	2°@10m / 6.3°@20m
1	1 ps	3 GW	890 mJ/cm²	0.4°@10m / 1.3°@20m
1	200 fs	10 GW	590 mJ/cm²	0.6°@10m / 1.9°@20m
2	400 fs	1 GW	600 mJ/cm²	2 @10m
2	1 ps	0.3 GW	450 mJ/cm²	2.6°@10m
2	1 ps	1 GW	1500 mJ/cm²	0.8°@10m

To take into account also the volume dilution effect some calculations have already been made for the 4GLS source [8]. In this study the damage thresholds obtained experimentally for normal incidence 12.7 eV-photons [3] have been rescaled for different energies and 5°-grazing angle of incidence. In particular, it was found that within the 10 – 110 eV range there is a multiplying factor ranging between 20 and 100 for the damage threshold of carbon and silicon. This means that the thresholds found for normal incidence are increased going to grazing incidence, even if the reduced penetration of the photons in the material is taken into account.

Together with the issue of mirror damage, damage induced by the radiation on different optical elements like gratings, slits, multilayer coatings, transmission beam splitter should be taken into account. As an

example, the radiation impinging on a diffraction grating hits the groove walls with angles reaching very large values (see Figure 8.2.1 as a guideline), up to quasi-normal incidence. The effect on the groove shape is still to be determined and proper studies and tests must be carried out in order to determine the best groove profiles. More generally, tests on the damage threshold for different optical elements are mandatory and must be performed to help selecting the most efficient optical systems for the beam transport.

8.2.3   Coherence

The measure of the spatial coherence of the beam can be made in several ways. While all these methods are invasive, fortunately, one can reasonably assume that the transversal coherence does not vary from shot to shot. Interference effects could be used to measure the transverse coherence length, possibly in the whole beam in a single shot (like in the Fizeau or Michelson experiments). In contrast, it is very difficult to preserve the coherence along a beamline, simply because the presence of non-perfect optical elements. If an high degree of coherence is necessary, the relevant optics must have a surface profile much better then what is requested for SR beamline. Residual slope errors in the order of 0.1 µrad (rms), including the holding effect, are necessary. This implies a substantial effort in metrology, probably including "at wavelength" metrology in a dedicated facility.

8.2.4   Beam Splitters and Filters

Several experiments require the splitting of the incoming beam into two beams for a further recombination (study of interference effects), or with the purpose of their relative delay for pump-probe experiments. The easiest way to split the beam at these energies is the use of a diffraction grating (Figure 8.2.4).
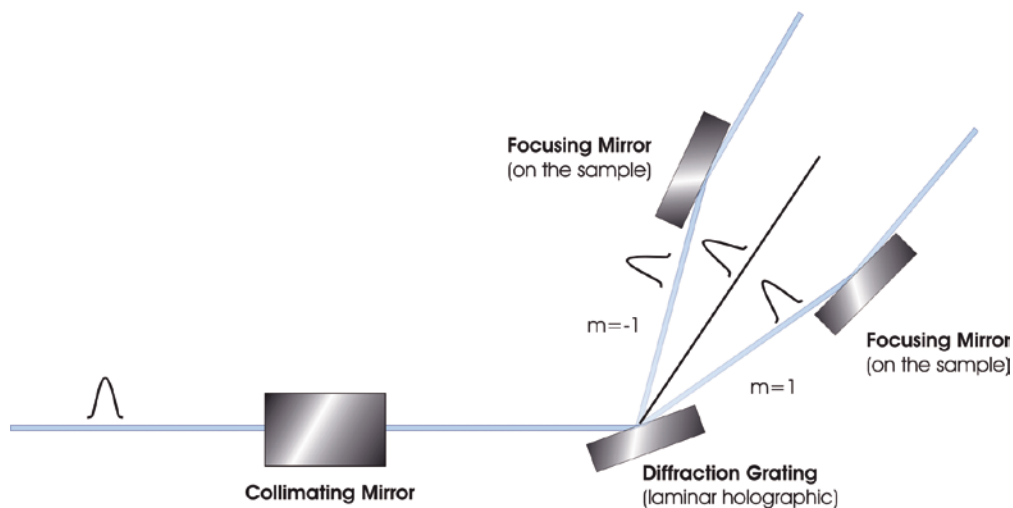

Figure 8.2.4:
Scheme of the beam splitter proposed for the time-resolved spectroscopy beamline (Masciovecchio, Ruocco, Sette, Torre).

The grating disperses the same wavelength at different diffraction orders including the zero order, which corresponds to the reflected beam. Several needs must (or could) be met: 1) splitting the beam at different directions but with almost the same intensity (if necessary), 2) avoiding temporal lengthening of the pulse (if necessary), 3) permitting the use of both beams within a wide energy range (the direction of the diffracted beam depends on the incoming wavelength). Nevertheless, optimizing case-by-case, possible solutions exist. Figure 8.2.4 presents a scheme planned for one of the beamlines proposed for FERMI@Elettra (Masciovecchio, Ruocco, Sette, Torre). In this case, the efficiencies of the +1 and –1 order are almost the same (17.5 and 17.8%).

Another option is the use of thin metallic foils that pass part of the radiation and reflect the remainder at a particular angle. This task is challenging because the metallic films, often used as filters, do not have surfaces as good as a mirrors. Moreover, they are easily damaged by the incoming peak energy. This approach as well as the use of multilayer optics requires further study. Regarding the filters, most of the work is done by the monochromators. With filters one can remove energies outside the central Gaussian peak from the optical spectrum.

Some experiments require suppressing higher harmonics or reducing their intensity. The latter task can be accomplished by using gas cells, with or without entrance and exit windows. Except for the determination of the proper gas mixture and pressure, cell design is not a significant problem (see section 8.3.1). This solution, in some cases, is also useful for suppression of higher orders, but multilayer mirrors or transmission filters are probably better. A detailed study of the filtering is foreseen during the conceptual design of the first approved beamline for FERMI@Elettra.

8.3 Optical Systems before the Beamlines

Several optical systems serve as interfaces between the FERMI@Elettra undulators and the experimental stations, performing many different functions. Besides the installation of the beamlines in the experimental hall (discussed in the next section – 8.4), other systems are inserted between the exit of the undulators and the first mirrors of the beamlines. These include differential pumping sections hosting gas I_0 monitors and absorbers, some kind of angular divergence defining systems (e.g. slits), and the very first mirrors of the beamlines acting as power absorbers and radio-protective elements.

8.3.1 Absorption Cell and I_0 Monitor

The FEL radiation is transported through a window-less system starting from the exit of the undulators. To host sections in which it is possible to perform gas absorption measurements, differentially pumped sections are inserted before the protective wall in front of the first mirrors. Here a double task can be accomplished: the attenuation of the FEL radiation intensity and the monitoring of its absolute intensity. The former is realized through the use of high-pressure noble gases that are pumped at a pressure of 0.1 mbar as an upper limit [9] into a 6-meter-long cell. Figure 8.3.1 reports the calculated transmission of this cell for different gases at pressures of 0.1 and 0.15 mbar in the spectral range 10 to 100 nm.
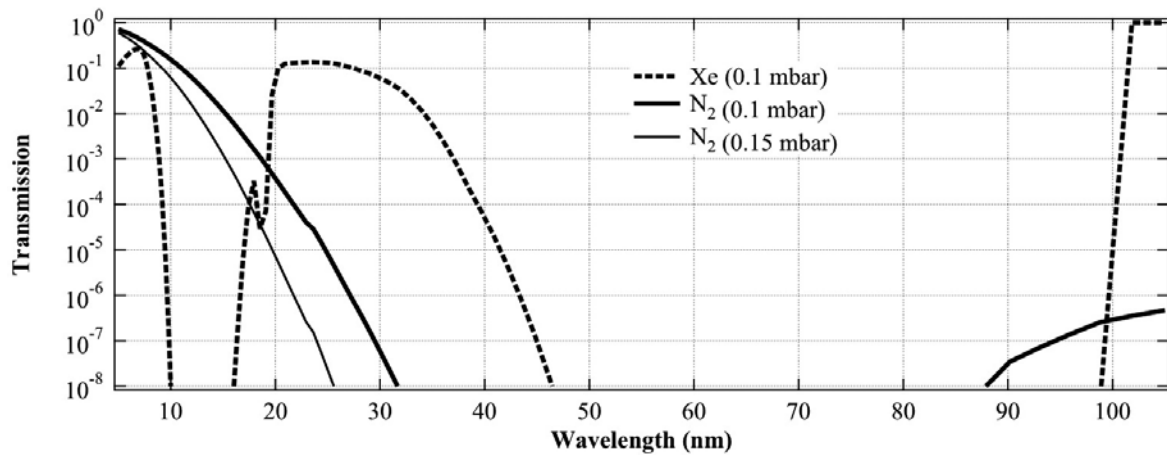
Figure 8.3.1:
Calculated transmission of the gas absorber for different gases and pressures (gas cell is 6 meters long).

It is clearly possible to attenuate the intensity of the FEL radiation by several orders of magnitude by selecting the proper gas. From about 20 to 100 nm nitrogen can be used, while between 19 and 9 nm xenon is preferred.

The second task to be accomplished within the differentially pumped section is the monitoring of the radiation intensity by a gas-monitor / detector, probably similar to that developed for the DESY FEL [10]. The monitor, based on atomic photoionization of a rare gas at low particle density ($P = 10^{-5}$ mbar), is free from degradation and almost transparent. Consequently, it is suitable for on-line measurements. Moreover it can simultaneously detect photo-ions and photo-electrons, and measure the absolute photon number per pulse.

Also within the same vacuum chamber, pairs of parallel plates are installed for beam position monitoring. This item is discussed in Section 8.6.3.

8.3.2   X-ray Slits

The FEL radiation emitted from the undulators entering the x-ray beam transport system consists of an intense coherent emission with a rms angular divergence of about 50 µrad for FEL-1, and 15 µrad for FEL-2, surrounded by a broad spontaneous distribution with a larger angular divergence. For some experiments the low energy spontaneous emission constitutes background noise that must be removed. Other experiments may require removing greater amounts of the off-axis radiation. These considerations impose the introduction of an element (collimator) to delimit angular divergence. The collimator has not yet been designed. Careful consideration and detailed calculations must be carried out to determine if it is possible to place horizontal and vertical double slits before the beamlines. These cannot be used for focused, undispersed FEL radiation due to the ablation effects on the jaws. Another possibility [1] is the

baffling of the grating, which can safely improve the pulse length without excessively deteriorating the energy resolution. Unfortunately, since baffling cannot reduce the effective source size, as an entrance slit would do, this method cannot improve the energy resolution if the beamline is limited by a large source size.

8.3.3   First Mirrors

Two plane mirrors (one for each FEL) are placed at the entrance of the experimental hall, still behind a protection wall. Their role is to deflect the FEL radiation by about 3° to prevent unwanted radiation (including bremsstrahlung, undulator x-rays and so on) passing through and traveling along the beamlines and/or in the experimental hall. As these mirrors also serve as power absorbers, much less energetic radiation is delivered to the more delicate, downstream optical elements, such as the variable line spacing (VLS) grating, located after the mirrors. As seen in Table 8.2.1, to prevent optical surface damage these mirrors are located at least 15 meters from the undulator exits, and work with an incidence angle of 1.5°. Very likely the coating material will be carbon or gold, due to their excellent optical characteristics.

8.3.4   Time Arrival Monitor

A system to monitor the arrival time of the photon pulses may be installed just after the undulator exit, close to the electron beam dump section. Here dipole radiation is emitted when the electrons are forced to bend away from the undulator axis and towards the beam dump. This radiation, in principle, can be used as a marker for the time arrival of the photon beam pulses into the optical systems (beamlines) since it is directly related to the electron bunch time arrival in the undulators. Different methods can be employed to measure the time arrival jitter. One option is to use an optical streak camera to measure the dipole radiation with resolution ~300 fs, thus giving good information about long-term drifts [11]. Another possibility is to employ electro-optical sampling of the electric field surrounding the ultra-relativistic electron bunch. This task is accomplished by monitoring the transient birifrangence of a crystal (like ZnTe) placed adjacent to the electron beam. In this way resolutions below 100 fs are achievable [12].

8.4   Beamline Design

The design of the photon beam transport system is the major task to be accomplished to fulfill the requests of the FEL users who work on the endstations. This work must take into account the various characteristics of the radiation such as pulse length preservation, monochromatization and energy resolution, source shifts compensation, focusing in the experimental chambers, beam splitting, and so on. Obviously, different beamlines will have different needs that cannot be fulfilled simultaneously, for example, short pulses and high energy resolutions. While a thorough design and description of the beamlines of FERMI@Elettra is still in progress, some conclusions about this issue may be already drawn.

8.4.1   Source Longitudinal Shift Compensation

The FEL radiation is generated in the final sections of the radiators used for FEL-1 and FEL-2, but the effective longitudinal position of the photon source is energy dependent; shifts as large as 5 meters are foreseen. If a small spot is required, it is probably necessary to employ adaptive focusing mirrors. Use of mechanical benders and piezoelectric bimorph mirrors [13] has been already made at ELETTRA with optics developed by SESO. If a homogeneous unfocused beam is required, the bimorph mirrors are preferable, although it still must be determined how close to the experimental chamber a non-bakable mirror (like this one) can be hosted.

Since the beam can move longitudinally, it is almost impossible to have a spot smaller then about 5-10 μm. In fact to have such a small spot the source would have to be de-magnified by a factor 20 or more, and the divergence would increase the same amount. A source distance change of X produces an image shift of X divided by the square of the demagnification. That means that r a demagnification of 20 and a beam movement of 2 meters produces an enlargement close to 10 μm. This demagnification cannot be compensated by adaptive optics, but it can be minimized by reducing the accepted beam divergence or by proper optical setup.

8.4.2   FEL 1-2 Switching Mirror Chamber

One of the main goals of the photon beam transport system design is the possibility of directing (not simultaneously) the radiation generated by either FEL into the same endstation(s). This requirement enables a broad range experiments without the need of moving the endstations in the experimental hall. To fulfill this requirement, a preliminary layout of the experimental hall with the beamlines has been realized (see Figure 8.4.1). The critical dimension is the distance between the two undulator sections from which the two FEL beams originate. This value, which has been set to 2 meters (Chapter 7 for details), imposes some limitations on the beamline design.

A reasonable solution is depicted in figure 8.4.1. The two parallel beams coming from the undulators are deflected by the first mirrors towards two VLS plane gratings used for diagnostics (see Section 8.6.1). The VLS gratings then send the zero order beams to the main switching mirror chamber. This chamber can re-direct each of the two incoming beams to the three following branch-lines, where the beamlines are realized. As a consequence, the chamber hosts four mirrors since in two cases the beams simply pass through it without need of deviation. Additional beam switching can be performed along the two external branch-lines following the 3-way switching chamber. In this way serving all the endstations depicted in Figure 8.4.1 with both FELs can be accomplished. A complete mechanical design must be

produced in the near future probably involving mirror exchange systems very similar to those typically used in the ELETTRA switching mirrors (see Section 8.5 for further details).
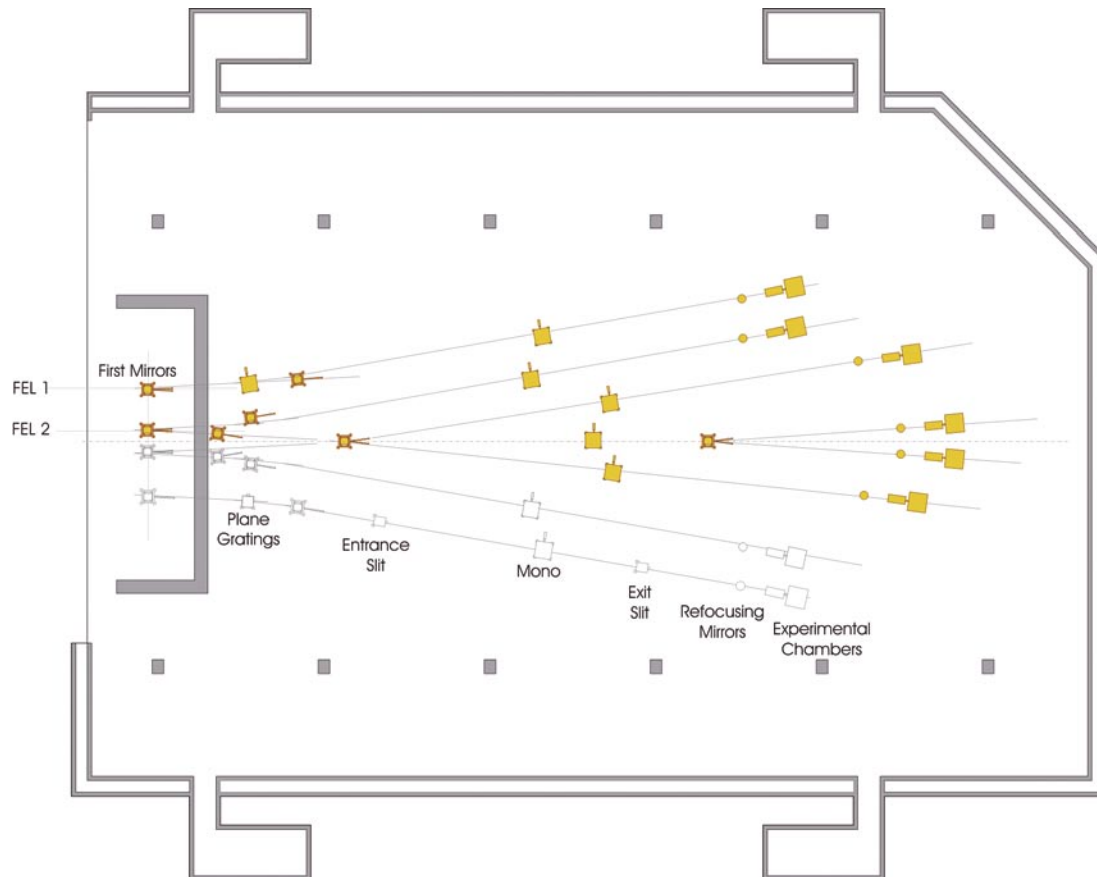

Figure 8.4.1:
Tentative layout of the experimental hall.

8.4.3   Monochromators

As already stated, some experiments/beamlines may need to stretch the bandpass delivered by the FEL at the cost of a pulse elongation. Consequently, monochromators must be installed along some beamlines to meet this requirement. They are based on diffraction gratings working at grazing angles of incidence, assuring low power densities on their optical surfaces. The use of diffraction gratings also helps in splitting the beam, when needed, due to their capability of diffracting the radiation in several orders, including the zero order (specular reflection). A comparative study of the several possible schemes has to be carried out to select the best solution for the different needs. In addition, monochromatized beams could produce without pulse elongation through the use of time preserving monochromators. These

instruments include two gratings working in opposite angle configurations to monochromatizes the pulse, while maintaining its original duration.

8.4.3.1 Traditional Schemes

In the energy range of FEL-1 the best monochromators operate at normal incidence. Unfortunately, the high energy density at FERMI@Elettra makes this solution impossible. A second design constraint is that the source distance changes for different selected energies. The ideal solution for compensating source distance variations is a variable included angle spherical grating monochromator (Padmore monochromator [14]), which gives the possibility of freely choosing the angles of incidence and diffraction, and consequently the position of the monochromator image. A plane grating with variable groove density [15] could work in a similar way and, in principle, produces less aberration in the final image, but it cannot provide a non-monochromatic focused beam. The SX700 (variable included angle plane grating monochromator [16]), with a collimating mirror before it and a focusing mirror after, could work properly but it involves four optical elements. A possible solution is the Dragon monochromator [17], for which the exit slit is movable to follow the variation of the focal distances for different energies. The beam can be refocused later on the sample by proper adaptive optics (see next paragraph). Therefore, several approaches can be used but the one least sensitive to beam instability, source movements, and that lets the beam pass through with the least disturbance must be preferred.

The major challenge is the realization of a system that cuts higher orders. In this energy range the efficiency of the second order of diffraction is still quite high as compared to the first one, even with a well-designed grating profile. It probably will be necessary to use filters, but this strongly depends on the level of higher harmonics produced by the undulators.

8.4.3.2 Time Preserving Monochromator

Most beamlines will use two monochromators, one with large band pass, used to "clean" the pulse from any photons with energy outside the central Gaussian peak, and one that selects a very narrow bandwidth.

For the first task, a coarse grating with few lines per millimeter (50 or less) is enough, considering that a bandpass of the order or 10 or more meV is expected. Such a grating has an effect only in the case of FEL-1, in which a pulse of about 100 fs is expected. Thereafter a grating with 33.3 lines/mm, suffices to select a 5-10 meV band pass, increasing the pulse length to 0.2-0.25 ps (Figure 8.4.2, left). Pulse stretching can be compensated by the use of a second grating with working angles inverted with respect the first one. In this case the rays that have traveled a longer path through the first grating will travel a shorter one in the second, and vice versa. In practice, on a case-by case basis, one must assess if it is better to "recompress" the signal, losing a factor 2 in intensity (grating efficiency in this energy range is not higher than 50%) or to use a slightly longer pulse.

In the case of FEL-2, when a 5-10 meV bandpass is required, it suffices to use a single grating, since the lengthening of pulse duration is negligible (Figure 8.4.2, right). In this case a 66.6 l/mm grating is used and an incoming pulse length of 0.5 ps is supposed.
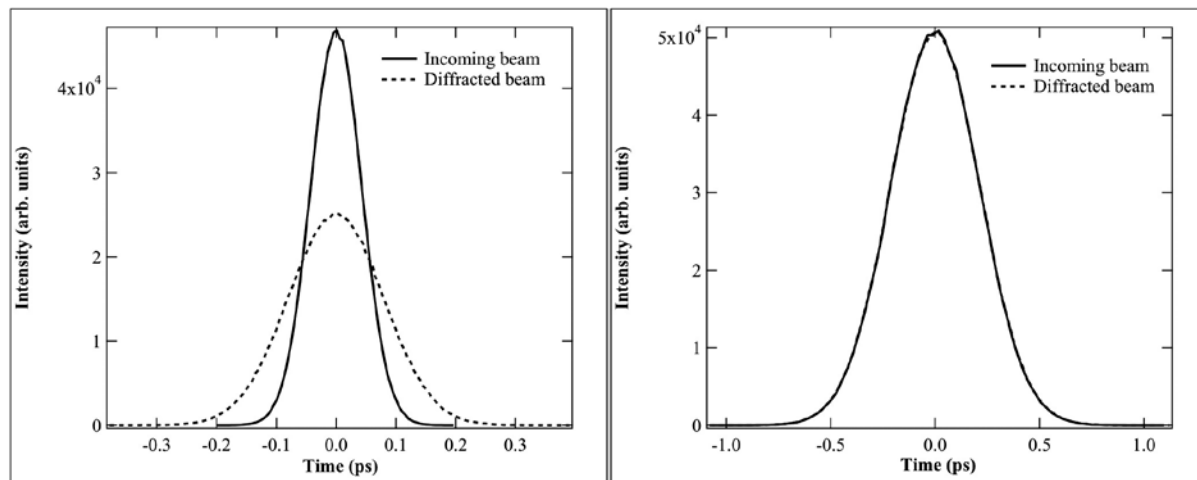
Figure 8.4.2:
Effect of the temporal lengthening of the pulse due to the monochromator to select a
energy band pass of 5-10 meV in the case of FEL-1 (left side) and FEL-2 (right). The
effect is similar in the whole energy range and is completely negligible for FEL-2.

When a high-resolution monochromator is needed in principle, the effect on the beam duration is more evident but it is probably possible to work below the transform-limited value (as in Figure 8.2.2). Therefore, in the design of a monochromator the temporal lengthening has to be taken into account. The proposed design should be optimized with respect to groove density and angle of incidence in such a way as to minimize this effect, avoiding stretching of the pulse beyond the transform limit.

A test of a time compensating double monochromator using commercial UV gratings made by Jobin Yvon is scheduled in the laser laboratory of ELETTRA where a 260 nm pulsed source is available. This is an almost costless test, performed to gain experience on the necessary precision, tolerances and practical problems related with the realization of a real time preserving monochromator.

8.4.4 Refocusing Optics

Refocusing sections are needed after the monochromators (when used) in order to focus the photon beam onto the samples in experimental chambers. Several optical designs may be used, depending on the spot sizes requested. These designs may include the use of single toroidal mirrors to refocus the beam in both horizontal and vertical directions, or the use of pairs of mirrors (spherical or plane elliptical) in a Kirkpatrick-Baez configuration (with the possibility to use adaptive optics if necessary). No major optical and technical problems are expected in the design and realization of these sections.

8.4.5 Experimental Stations and Related Equipment

Typically, experimental stations are placed at the end of each beamline. Independent of the details of the experiments to be performed, sufficient room is needed around each experimental station to allow the

installation of the experiment-related instrumentation such as optical tables, preparation and sources chambers, transfer lines, racks for electronics, pumping stations and so on. To achieve this goal the optical design of the beam transport system includes planar optical elements to separate the different beamlines as much as possible.

Pump-probe experiments will require a reference signal supplied to the endstations including information about the time arrival of the single pulses. For this purpose an optical signal derived from the seeding laser will transported to the endstation and used to select the optimal timing set-up.

8.5   Mechanics

This section provides an overall layout and a preliminary design of the beam transport and diagnostic system. Particular attention is paid to those elements that differ from or are more critical to experimental performance than those developed for the ELETTRA beamlines.

8.5.1   Layout

The overall layout of the beam transport and diagnostic system (Figure 8.5.1), based on the optical scheme described in paragraph 8.4 (Figure 8.4.1), accounts for the considerations described in the previous sections.
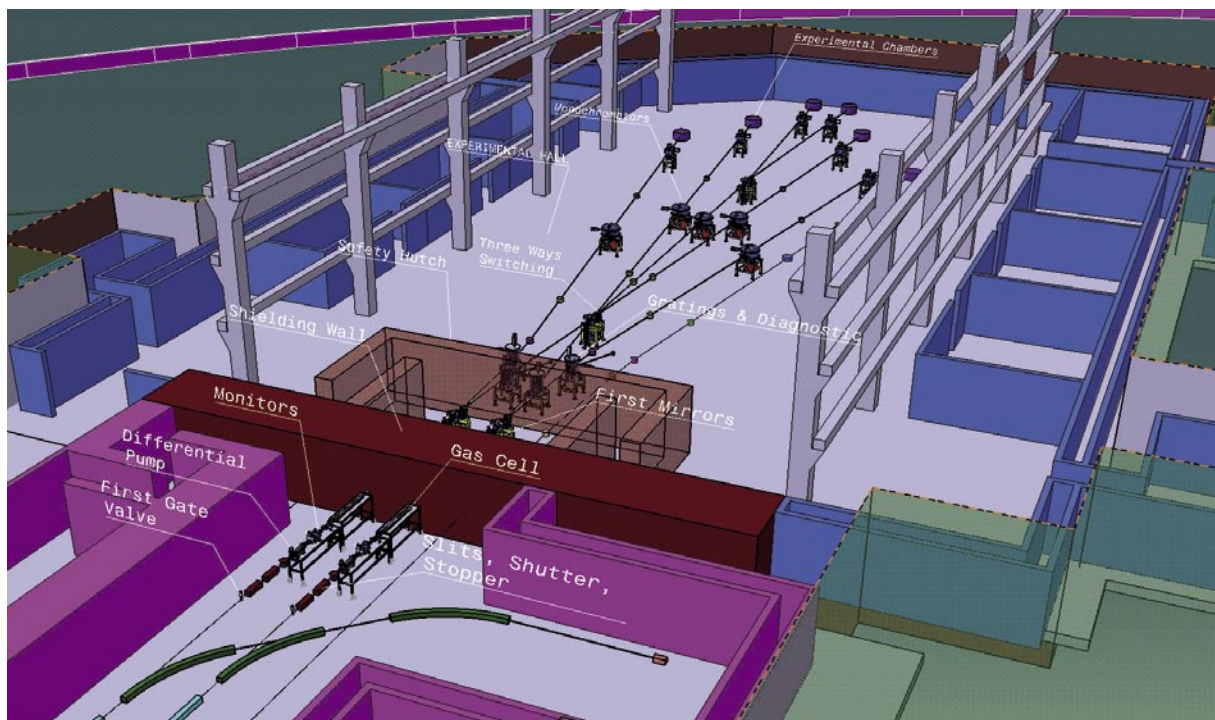

Figure 8.5.1:
Preliminary beamline layout and experimental hall.

The 3D beamline skeleton consists of a set of cylinders with a vertical axis representing the vacuum vessels containing a generic optical element (point of interaction between the photon beam and any optical surface); the cylinders are connected to each other by pipes with the horizontal axis representing the beam path with the proper angles in the point of intersection. This simple scheme is adopted for efficiency using the Sincrotrone Trieste CAD system. The choice of a relatively small number of parameters (FEL axis distances, position of the chambers along beam axis, grazing angles) makes it possible to reflect the optical layout updates (within the basic scheme) in a slim and fast model. The skeleton is then "dressed" by positioning the proper chambers substituted for the vertical cylinders and covering the "beam pipes" with the proper vacuum elements (chamber, valves, etc.) as the mechanical design proceeds.

In practice it is neither possible nor desirable to freeze the layout of the beam transport and diagnostic system at the outset. In fact during the initial commissioning of the facility not all the beamlines will be installed and or ready for use. Therefore the layout is constructed as 1) a basic tool to drive any further development of the overall system, and 2) to anticipate all the necessary space for building and plant layout from the very beginning.

In Figure 8.5.1 the optical scheme is reproduced in true dimensions, and an external beamline coming out from a possible additional undulators chain (say FEL-3) is included to account for future developments.

The layout study has proceeded by recognizing those beamline elements already working in 3rd generation synchrotron beamlines that can be customized for the new beam transport and diagnostic system. Particular attention has been dedicated to those elements that will be common for the future beamlines. These elements (Switching, Gratings and Diagnostic, etc.) are described in the next sections, and the associated models provide the mechanical schemes for the final design. In other cases the simplified CAD models (Prefocusing, Refocusing, Monochromators, Slits, etc.) are simply elements extrapolated from present applications that look "reasonable" even for future application. They are put into the layout to gain understanding of the relative position and the possible interferences between the beamlines with realistic models. Moreover, the resulting layout is useful for understanding how to develop the auxiliary systems, i.e. cooling piping, electrical cabling (both power and signals), pneumatic systems, etc., and the basic schemes for the overall vacuum system.

8.5.2   Experimental Hall

The mechanical layout of the overall beamline transport and diagnostic system scheme drives some of basic system requirements the buildings and plant installations, (see Chapter 14). The FERMI@Elettra photon source will be constructed using the existing LINAC, presently used as pre-injector of the ELETTRA storage ring. The LINAC will be modified for the new FEL application but the basic structure in the present position is preserved, i.e. the electron beam axis is -3.9 m underground (LINAC floor -4.75 m), with respect to the conventional ground zero level (Elettra experimental hall). Since maintaining high beam quality limits the electrons optics to small angles of deflection, to the FEL layout avoids vertical deflections that imply very long slopes before the undulator sections. As a consequence the experimental hall itself is constructed underground, since the photon beam has the same level. For the experimental hall the distance between the floor and the photon beam has been increased to 1.3 m (vs. 0.85 m in the LINAC tunnel), i.e. the resulting floor is -5.2 m under ground level.
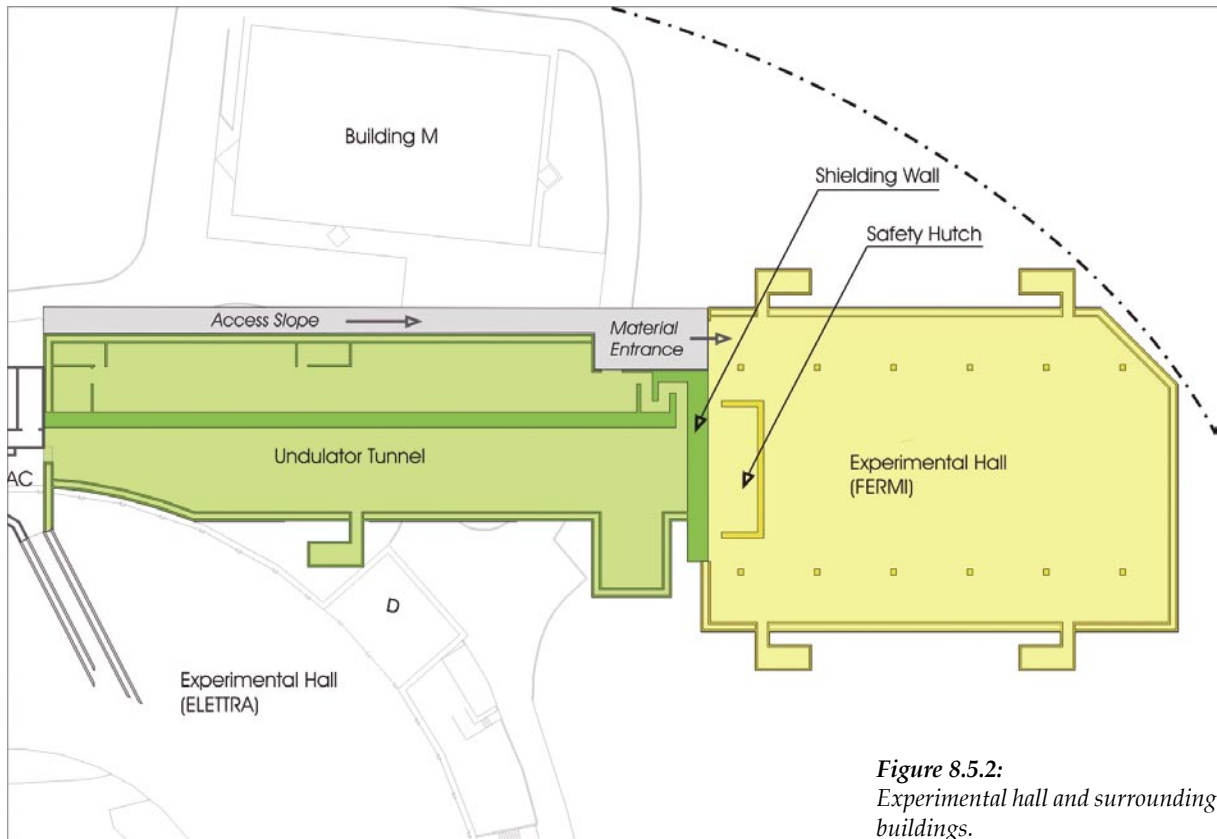
Figure 8.5.2:
Experimental hall and surrounding buildings.

The overall dimensions of the experimental hall are approximately 60×40 m (L×W), and its position with respect to the absolute axis system (origin in the ELETTRA storage ring center, x-axis parallel to LINAC direction, z vertical) is described in Figure 8.5.2. In this picture the relative position of the experimental hall with respect to the surrounding buildings is also visible. The experimental hall is separated from the undulator tunnel by a 3 m-thick concrete wall as a primary safety radiation protection element. The first-mirrors chambers (switching mirrors) are placed in the Safety Hutch since the role of these mirrors is to absorb the main heat load and to deflect the photon flux (3°) while the residual gas-bremsstrahlung (0°) is absorbed by the next concrete wall. The lateral walls of the Safety Hutch are about 800 mm-thick and the access is through a labyrinth. Therefore, to permit installation and maintenance access, the roof consists of removable blocks permitting the use of a crane for handling the devices and the roof blocks themselves.

The Experimental Hall area is divided into three parts by two rows of pillars that have the primary function of supporting the crane system for the beamline chamber installation and handling. All the beamlines are placed in the 26 m wide central zone. The width is set by the consideration that, in the present conceptual layout, the distance between the external experimental chambers is about 20 m. In analogy with the ELETTRA Experimental Hall, the height of the crane railways is about 8 m and therefore the height of the overall building is about 10-11 m (at least in the central area between the

pillars). Since the Experimental Hall floor is -5.2 m from zero level, about one half of the building will be underground.

The two external areas delimited by the rows of pillars are useful space for auxiliary beamline laboratories (mechanical and electrical pre-assembly and testing, vacuum lab, experimental chambers lab, etc.) and general systems (cooling, pneumatic and electric systems).

All of the described dimensions will be optimized in the final design drawings.

8.5.3 Switching Elements

The Switching Mirror Chamber (SMC) is a key element in the layout of the photon beam transport system since, as already outlined in paragraph 8.4.2, one of the main tasks of this system is to redirect the photons of both FELs to the maximum number of possible beamlines.

The basic switching scheme is described in Figure 8.5.3. Three SMCs feed five beamline branches (BL1 ÷ BL5). SMC1 and SMC2 are the chambers in which the first mirrors (two mirrors per each chamber) are
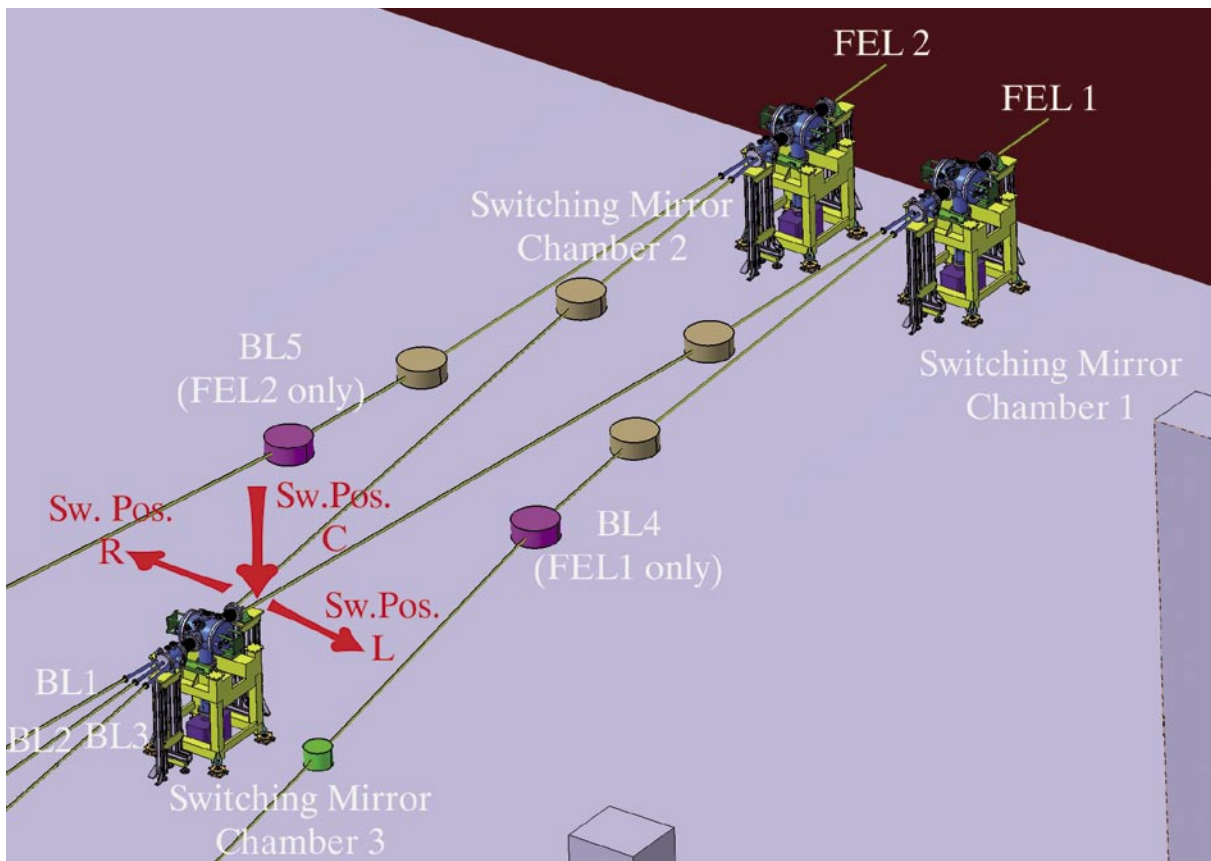

Figure 8.5.3:
Photon beam switching scheme.

placed and which receive the photons from FEL-1 and FEL-2 respectively. As the function of these two chambers is similar to that of many other switching chambers at ELETTRA beamlines, the mechanical scheme is derived from these devices. The switching function is obtained by a horizontal translation (perpendicular to the beam) of the whole chamber. In the two possible positions (left and right position) the center of the respective mirror is aligned with the photon axis.

Each mirror has two angular degrees of freedom (pitch and roll) controlled by a manipulator similar to the one described in Figure 8.5.4. The manipulator axis (and therefore the connection flange) is inclined at 90°+ α (where α is the grazing angle of the mirror) in the horizontal plane with respect to incoming beam direction. Theoretically the two translation movements are enough to obtain the ± 2α beam deflection, while the pitch and roll controls are used for the fine alignment of the beam.

When the beam is deflected through the central part of the layout, photon flux distribution over three different beamline branches is required. Hence, the switching device (SMC3) must have six switching positions (three beamline output per each FEL photon input) instead of the two switching position required for SMC1 and SMC2. In SMC3 two of these six connections are simply realized by adding a central position to the chamber (neutral position). In this situation the photon beam coming from both FEL-1 and FEL-2 simply runs through the chamber and connects FEL-1 to BL1, FEL-2 to BL3. Once the SMC3 is in left or right position, two different angles of deflection are required. This second switching degree of freedom is obtained by controlling the pitch of the mirror through the manipulator. In the present layout the two required defections are $2\alpha_1 = 5°$ (FEL-1→BL2, FEL-2→BL2) and $2\alpha_2 = 10°$ (FEL-1→BL3, FEL-2→BL1).

For the manipulator to have a symmetrical behavior through the pitch angle travel, the manipulator axis must be inclined by $90+\alpha_m$ (where α_m is the average between α_1 and α_2) in the horizontal plane with respect to the incoming beam direction. The total range of the pitch control must exceed $(\alpha_2 - \alpha_1) = 2.5°$ to have some residual pitch control in the two extreme positions.
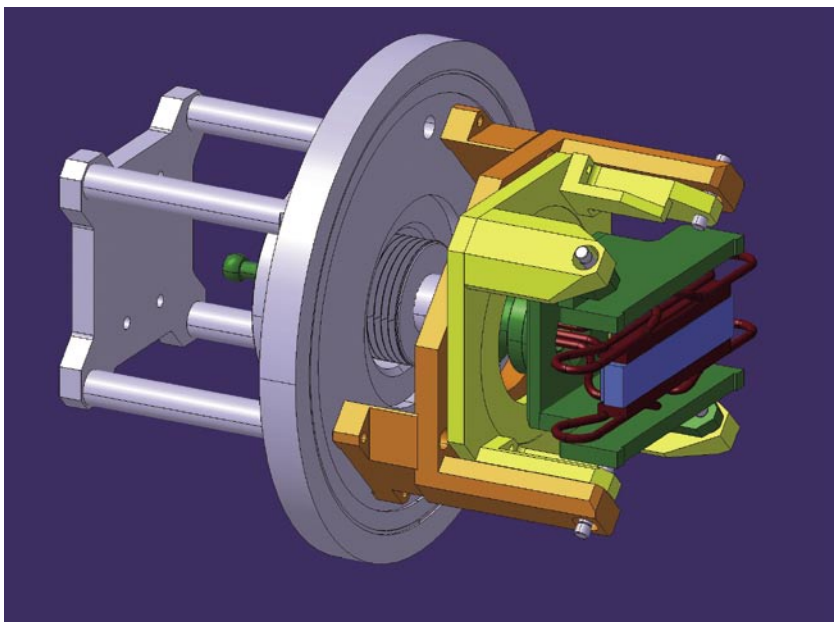

Figure 8.5.4:
Switching mirror manipulator.

In the present layout scheme each of the two FELs photon beams can feed four of the five planned beamline branches (Figure 8.5.3). Furthermore, the switching mirror scheme can be used to split again each branch line, if an increased number of beamline is required.

8.5.4   Gratings and Diagnostics Elements

One of the advantages of the present photon beam transport system layout is the possibility to concentrate the diagnostic system, common for all the beamlines, in the first part of the layout scheme, just after the first mirrors, and outside the safety hutch. The next section describes the physical principles of the diagnostic system and presents an overview of a preliminary mechanical scheme.

The gratings and diagnostic system are positioned between the first mirrors (SMC1 and SMC2) and the 3-way switching chamber (SMC3), just outside the 800 mm thick wall of the safety hutch. In Figure 8.5.3 the grating chambers are respresented as brown cylinders. In Figure 8.5.5 the cylinders are replaced by the proper vacuum vessels, in which the grating manipulator is visible in transparency.
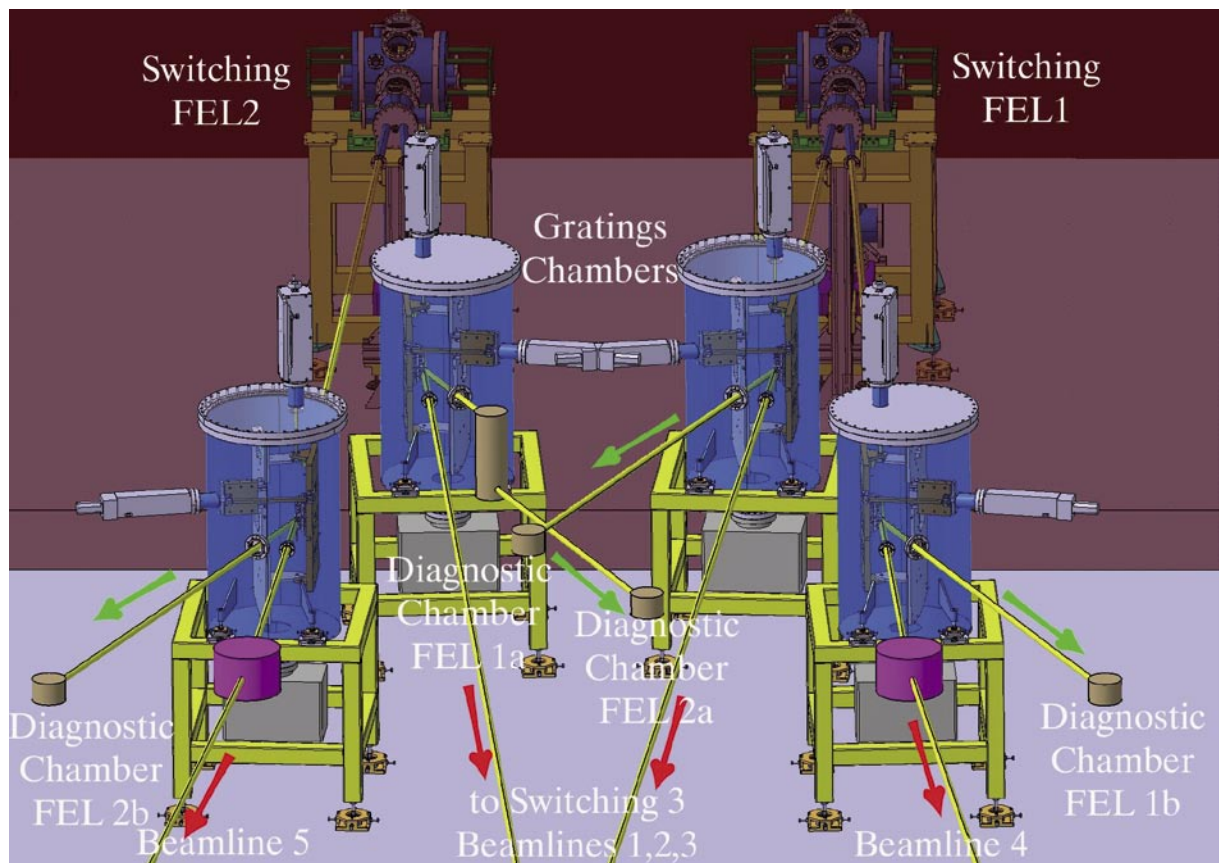

Figure 8.5.5:
Beamline diagnostics layout.

The two upstream switching chambers are also visible in transparency, otherwise hidden by the shielding wall of the safety hutch.

In each of the four chambers the proper plane grating deflects the zero order beam to the beamline branch (red arrows), while the first order (green arrows) is measured by a linear or bi-dimensional detector mounted in the small brown vacuum vessels of Figure 8.5.5. Each of these elements is connected to the grating chambers with bellows, and mounted over a motorized X-Y linear stage. These additional degrees of freedom permit positioning the detector at different angles with respect to the grating (transverse movement Y), and with different distances with respect to the grating itself (longitudinal movement X, along beam direction). A critical location for the diagnostics system is that of the two internal grating chambers where the first order beams intersect (diagnostic chamber FEL-1a and FEL-2a). To avoid the intersection of the two devices a periscopic chamber (two plane mirrors) is placed along one of the two diagnostic lines (FEL-2a in the Figure 8.5.5).

In the gratings chamber the gratings are mounted on a vertical sliding system that allows the grating selection for the proper energy range. The translating system can then rotate around the same translation axis and the rotation (pitch control) is driven by the crank gear. By moving the stage in the horizontal direction it is possible to finely control the pitch of the active grating, and therefore the beam deflection.

8.6 Photon Beam Diagnostics

Several characteristics of the emitted radiation can be measured. Some of these measurements must be highly reliable and precise, possibly shot by shot, so that the experimentalist can use the information to normalize their data. The same or similar information is useful for machine physicists to improve the performance of the FEL. The photon diagnostics are developed to satisfy the requirements of both the users and the machine physicists. Some photon beam characteristics, such as polarization degree, background to peak ratio, energy vs. time distribution (chirp) could be useful but their measurement is difficult. As they are not considered critical, the design of such diagnostics is left for the future.

The different diagnostics employ state-of-the-art instrumentation (eventually with a limited in- house modification), and maintain the option of upgrade based on internal or collaborative research and development.

8.6.1 On-line Energy Spectrograph

The photon spectrograph is an on-line device able to measure, shot-by-shot, the energy profile and consequently the relative intensity of each incoming pulse. Since each undulator can feed more than one beamline, to avoid duplication of instruments the first part of each beamline will be constructed as in Figure 8.6.1.
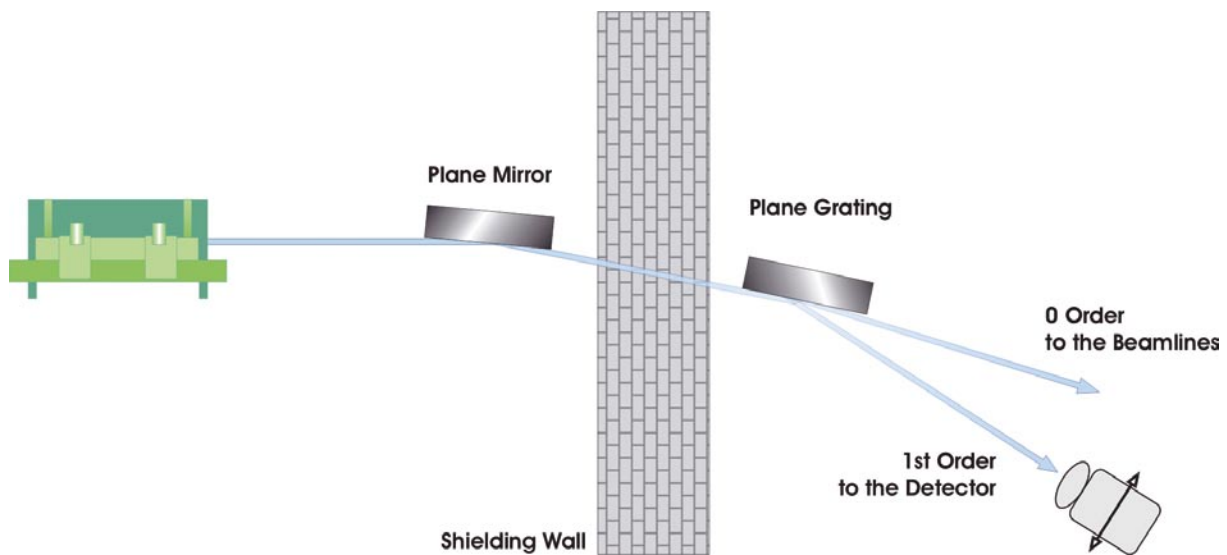
Figure 8.6.1:
Layout of the photon transport system from the undulator to the diagnostics.

A first plane mirror (used only for safety reasons) deflects the beam outside the shielding wall. Just outside the wall, a plane VLS grating deflects the zero order to the beamlines and the first order to a linear or bi-dimensional detector. The advantage of using a plane VLS grating is twofold: no further optics are needed to focus the beam on the detector, and the beam passes trough the instrument (via the zero order) without altering its divergence.

In principle the VLS grating could also be positioned before the shielding wall, but there are two major advantages of having it outside. The first is related to long-term deterioration, which is much less critical for a mirror than for a grating, from the optical point of view. Consequently it is better to place the mirror upstream of the grating. If excessive power arrives at the first element and damages it, a plane mirror is cheaper to replace than a VLS plane grating. The second advantage is the possibility to have the spectrograph (that can be about 3 meters long) completely outside the wall, with easy access for alignment, calibration, and so on. The disadvantage is the additional reflection that does not significantly alter the intensity of the beam (reflectivity > 95% is expected in the whole range) but can degrade the beam quality.

The VLS grating focuses different energies in different positions, and a position-sensitive detector collects the photons, transforming a spatial distribution into an energy distribution. Since the expected energy width of the beam can be lower than 10 meV, the spectral profile must be defined with a precision about 1 meV. This is not a problem for FEL-1, where a possible solution is the use of two gratings covering the whole energy range, providing resolution of the order of 0.2-0.5 meV, using a 13 μm-spatial resolution detector. For FEL-2, working at higher photon energies, the ultimate resolution reaches values about 5 meV. The system works with a fixed VLS plane grating and with a movable detector. Since the expected photon flux is quite high, the grating profile is optimized to deliver as much flux as possible in the zero order, and less then 1% in the diffraction orders.

Up to date it is not possible to collect a bi-dimensional detector image with enough dynamic range (16 bits) with a repetition rate of 10 or 50 Hz (value for FERMI@Elettra). In contrast a linear array detector can be read even with a higher repetition rate. The FERMI system therefore adopts a linear array detector (back illuminated or front illuminated with a proper phosphor coating) to measure the beam shot by shot, and a bi-dimensional detector placed close to the former, which measures one shot each 10-20 pulses triggered by a mechanical shutter.

8.6.2   Off-Axis Photon Beam Characterization

A second measurement of interest is determining the beam profile outside the central emission cone, to check the alignment and tuning of the undulators. This measurement is, in principle, quite easy using a standard, bi-dimensional, back illuminated CCD such as the one used for the spectrograph. In this way the radiation emitted at different angles with respect to the undulator axis is collected at different CCD rows. Moreover there is no need to collect images shot to shot, but simply to acquire averaged information over longer periods (e.g. seconds).

8.6.3   Position Sensitive Detector

To determine and control the spatial position of the photon beam along its path to the experimental stations, several position sensitive detectors are installed. These devices should provide information about both horizontal and vertical directions, monitoring spatial shifts of the beam in time. A possible design for this kind of instrument uses parallel plates in a gas atmosphere to collect the signals from gas ionization. Both electrons and ions can be collected, similar to the system successfully tested and employed in the FLASH FEL source in DESY-Hamburg [9]. This system is able to characterize the position of the beam with an accuracy of about 20 µm. The position sensitive detector can be mounted close to the gas absorbing section placed between the undulators and the first optical elements of the beamlines. Other more conventional beam position monitors can be installed and used along the beamlines themselves. They include fluorescent screens and metallic plates (both offline) for alignment, photodiodes for quantitative indications about beam shifts (off- and on-line), slit-pair systems (online) to monitor the beam alignment and eventually to correct it with a feedback procedure.

8.6.4   Photon Pulse Duration Characterization

Depending which FEL is used, different pulse lengths are delivered to the beamlines. In particular, FEL-1 delivers pulses of about 100-200 fs (FWHM), while FEL-2 delivers pulses of ~500 fs (fresh bunch mode). In order to characterize these lengths some instrumentation must be developed. The main difficulty is that to date no direct online measurements of this quantity are possible with sufficient time resolution. Streak cameras working in the EUV and soft x-ray regimes are capable, at the best, of resolutions around 500 fs [18] [19]. Other destructive (*e.g.* offline) methods exist for measuring the pulse length, such as auto- or cross-correlation techniques involving the use of ultra-fast lasers with short and well-defined pulse durations.

Initially invasive (not shot-to-shot) measurement of pulse lengths will be performed with cross-correlation techniques, with a precision of about 100 fs or less. Eventually, measuring the same quantity on-line, shot-to-shot, with a precision of the order of 200-250 fs may become possible by means of a streak camera. Experimental studies carried out at Lawrence Berkeley Laboratory (H. Padmore and co-workers) demonstrate the future feasibility of this kind of measurement. Active collaboration with this group is under way.

8.7   References

[1]   BESSY FEL Technical Design Report (2004).

[2]   LCLS Design Study Report (1998).

[3]   HASYLAB annual report (2001).

[4]   Y. Dong et al., *Appl. Surf. Sci.* **252**, 352 (2005).

[5]   D. von der Linde et al., *Appl. Surf. Sci.* **154-155**, 1 (2000).

[6]   H. Jeschke et al., *Appl. Surf. Sci.* **197**, 839 (2002).

[7]   H. Jeschke, et al., *Appl. Surf. Sci.,* **197-198**, 107 (2002).

[8]   4GLS Conceptual Design Report (2006).

[9]   K. Tiedtke et al., *AIP Conference Proceedings* **705**, 588 (2004).

[10] M. Richter et al., *Appl. Phys. Lett.* **83**, 2970 (2003).

[11] S. Düsterer et al., XFEL 2004 Workshop, Stanford (2004).

[12] H. Schlarb et al., *Proceedings of EPAC 2004*, 345 (2004).

[13] R. Signorato at al., *J. Synchrotron Rad.* **5**, 797 (1998).

[14] H.A. Padmore, *Rev. Sci. Instrum.* **60**, 1608 (1989).

[15] D. Cocco et al., *Proceedings SPIE* **3767**, 271 (1999).

[16] H. Petersen, *Opt. Commun.* **40** (1982).

[17] C.T. Chen and F. Sette, *Rev. Sci. Instrum.* **60**, 1616 (1989).

[18] J. Liu et al., *Appl. Phys. Lett.* **82**, 3553 (2003).

[19] Z. Chang et al., Univ. of Michigan, USA.

Table of Contents